Analytical Methods

Accepted Manuscript

FULL PAPER

Electrosensing of an alpha-adrenergic agonist psychoactive methyldopa using sodium bentonite-graphene oxide nanocomposite[‡]

Nagappa L Teradal[a], Prashanth S Narayan[a], Jaldappagari Seetharamappa[a]*, Ashis K Satpati[b]

In the present report, we describe the preparation of sodium bentonite-graphene oxide nanocomposite for electrosensing of methyldopa (MD). The fabricated electrode materials viz., graphene oxide (GO), sodium bentonite-graphene oxide (Bent-GO) and Bent-electroreduced graphene oxide (Bent-ErGO) were characterized by XRD, FTIR, absorption, Raman, FESEM and AFM methods. Bent-GO suspension was
10 prepared by exfoliation of GO and Bent in water. Bent-GO suspension was drop casted on GCE followed by electrochemical reduction to obtain Bent-ErGO/GCE. Electronic properties of modified GCEs were evaluated employing CV and electrochemical impedance measurements. Redox response of MD increased significantly with the negative shift in peak potentials at Bent-ErGO/GCE compared to that at bare GCE. Based on enhanced electrochemical response, chronoamperometric and differential pulse
15 voltammetric (DPV) methods were developed as alternative analytical methods for the assay of MD. Under optimized conditions, a linear relationship was observed between the peak current and concentration of MD in the range of 1.13 - 40.6 μM and 0.1 - 60 μM for chronoamperometric and DPV methods, respectively. Furthermore, the proposed electrochemical sensor was successfully employed for the determination of MD in pharmaceutical formulations.

20 Introduction

Graphene, a single-atom-thick and two-dimensional carbon material, has aroused enormous research interest and activity in the field of science and technology because of its unique features viz., high surface area, unusual electrical, chemical, optical, 25 mechanical and thermal properties [1]. The presence of functional groups like epoxide, hydroxy, ketone and carboxylic acid on GO makes it hydrophilic in nature. Its larger surface area and high conducting nature makes it as a suitable material for the fabrication of modified electrodes [2, 3]. In particular, reduced 30 GO (rGO) has been extensively used as an electrode material for electrochemical studies and analytical applications because of its excellent electronic properties [4-6]. Very low energy dynamics of electrons made the use of graphene attractive in electronics and electrochemical field. The sp^2 hybridized carbon in graphene 35 behaves like zero band gap semiconductor and exhibits interesting properties like quantum Hall effect at room temperature and the electrons behave like mass less Dirac fermions [7,8]. In chemical synthesis, GO is generally reduced to retain its aromatic backbone and to increase its electronic 40 properties. GO can be reduced by different methods including chemical [9-11], thermal and electrochemical [12, 13]. Among the reported procedures, the electrochemical method is a promising route for the reduction of GO. Hence, it has attracted enormous amount of research interest due to its green nature [14,

45 15].

Sodium bentonite (clay), a layered aluminosilicate clay mineral with a layer thickness of 1 nm, exhibits excellent intercalation properties for swelling, strong adsorption and ion exchange. So, it has attracted many electrochemists for the 50 modification of electrode surface for analytical applications [16].

Methyldopa, chemically known as (2-amino-3-(3, 4-dihydroxyphenyl)-2-methylpropanoic acid), is widely used in the treatment of mild to moderate hypertension. Its antihypertensive action appears to be due to stimulation of central adrenoreceptors 55 [17]. Various analytical methods including electroanalytical, flow injection spectrophotometric, kinetic and chromatographic methods have been reported for the determination of MD in pure, pharmaceutical formulations and biological samples [18-27]. In the present study, nanocomposite, Bent-GO was prepared, 60 characterized and electrochemical reduction procedure was adopted to obtain Bent-ErGO for sensing of MD. This was successfully used for the determination of MD in pure and pharmaceutical formulations. The results of the proposed method were compared with those of reported methods (**Table 1**).

65 Experimental

Materials

A stock solution of 1 mM MD (obtained from Reddy's Laboratories Pvt. Ltd., India) was prepared in Millipore water and stored in a refrigerator at 4 ºC. Working solutions of MD were

prepared by appropriately diluting the stock solution with phosphate buffer solution (pH 3 -10).

Table 1 Comparison of linearity range and detection limits of the proposed sensor with those of reported methods.

Electrode	Method	Linearity, μM	LOD, μM	Ref.
CA/BMI.N(Tf)$_2$/CP[a]	SWV[1]	34.8– 370.3	5.5	18
TR/SWCNTs/GC[b]	DPV	0.1 – 5.0	0.02	19
PPy/CNP/GC[c]	DPV	0.2 – 50.0	0.06	20
ILs/MWCNTP[d]	DPV	0.4 – 400.0	0.1	21
PPyox/NFR/Au[e]	DPV	0.1 – 20	0.05	22
FCCNP[f]	SWV[1]	0.1 – 400	0.08	23
p-CAMCNTP[g]	SWV[1]	0.5 – 165.5	0.2	24
Bent-ErGO/GC	DPV	0.1 – 60.0	0.04	Present work
	Chrono	1.13-40.6	0.96	

[1]Square wave voltammetry
[a]Cellulose acetate (CA) and ionic liquid, 1-butyl-3-methylimidazolium bis(trifluoromethylsulfonyl) imide (BMI·N(Tf)$_2$) modified carbon paste electrode
[b]Tyrosinase/single-walled carbon nanotubes/glassy carbon electrode
[c]Polypyrrole/carbon nanoparticle/ glassy carbon electrode
[d]Ionic liquid/multiwall carbon nanotubes paste electrode
[e]Poly pyrrole /nuclear fast red /gold electrode
[f]Ferrocene /carbon nanotube paste electrode
[g]p-Chloranil modified carbon nanotubes paste electrode

Apparatus

A CHI-1110a Electrochemical Analyzer (CH Instruments Ltd. Co., USA, version 4.01) was used for electrochemical measurements. Bent-ErGOGCE or bare GCE (3 mm diameter), a platinum wire and an Ag/AgCl were used as the working, counter and reference electrode, respectively. GCE was polished using 0.3 micron Al$_2$O$_3$ prior to each measurement. After polishing, the electrode was rinsed thoroughly with Millipore water and then subjected to modification steps. This procedure ensured reproducible results. The experimental conditions maintained for DPV were as follows: pulse amplitude - 50 mV; pulse width - 30 ms and scan rate - 20 mV s^{-1}.

EIS measurements were carried out on a potentiostat/galvanostat Autolab 100 with FRA software. Experiments were carried out by applying sinusoidal signal of amplitude 10 mV and the frequency in the range of 10 kHz to 0.1 Hz.

Material characterization

X-ray diffraction system, Philips X'Pert (Cu K$_\alpha$, 1.5406 Å) was used to study the crystalline structure of graphite and graphite oxide. The morphology of nanocomposites viz., GO, Bent-GO and Bent-ErGO was investigated using a Carl Zeiss, Ultra 55 field emission scanning electron microscope (FE-SEM). Further, atomic force microscopy (AFM) experiments were carried out on a flex AFM system, Switzerlands. Well dispersed nanocomposites were drop casted on a carbon tape and pristine mica sheet for FESEM and AFM measurements, respectively.

Preparation of sodium bentonite (Bent)

Sodium bentonite was prepared by stirring the dispersion of untreated bentonite in 1 M NaCl solution for 24 h. The dispersion was filtered through a Buchner funnel and rinsed with Millipore water until it was free from Cl$^-$ ions. The obtained sodium-enriched bentonite was dried at 110 °C. The dried Bent was used to prepare composite with GO [28].

Synthesis of GO and Bent-GO nanocomposite

Graphite oxide was synthesized from graphite powder by following the Hummers method [29]. Prepared graphite oxide (2 mg) was dispersed in 2 mL of Millipore water and sonicated in an ultrasonic bath for 2 h to obtain a stable suspension of graphene oxide (GO) .

Nanocomposite, Bent-GO was prepared by exfoliating 0.75 mg of graphite oxide and 0.25 mg of Bent in 1 mL Millipore water and sonicated for an hour to obtain a stable homogeneous suspension of Bent-GO [30].

Fabrication of ErGO/GCE and Bent-ErGO/GCE

ErGO/GCE was prepared as follows: initially, 5 μL GO suspension (1 mg mL^{-1}) was deposited on the surface of GCE and then it was electrochemically reduced by employing CV in the potential range of 0.7 to -1.6 V (ESI, Fig.S1†) [31]. Similarly, Bent-ErGO/GCE was prepared by the deposition of Bent-GO suspension followed by electrochemical reduction in the above said potential range [**Scheme 1**].
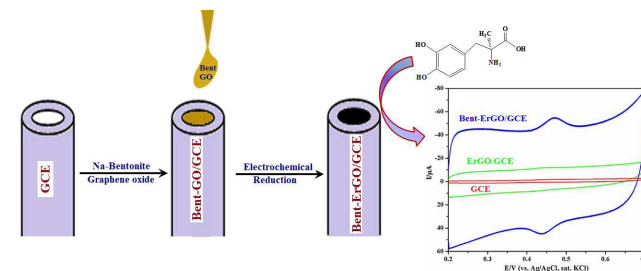
Scheme 1 Graphical representation for the fabrication of the proposed sensor, Bent-ErGO/GCE.

Assay of MD tablets

Tablets of MD (each containing 250 mg MD) were obtained from local commercial sources. Ten tablets were finely powdered, and a portion of this powder equivalent to 1 mM of MD was weighed and transferred into a 10 mL volumetric flask containing Millipore water. It was then sonicated for 15 min to effect complete dissolution, and diluted to volume with the same solvent. Suitable amounts of this solution were taken and analyzed. The amount of MD in the tablet was calculated using the calibration graph or regression equation.

Results and discussion

Characterization of GO, Bent-GO and Bent-ErGO

Powder XRD patterns of pristine graphite powder and graphite oxide are shown in **Fig. 1A**. Intense crystalline reflection at 26.66° (a) represents the hexagonal graphite with a d-value of 0.34 nm. Upon the conversion of pristine graphite to graphite oxide, a new reflection was noticed at 10.08° (b) and the corresponding basal spacing increased to 0.87 nm. Increased d-value was attributed to the intercalation of oxygen containing functional groups and water molecules in between the graphene layers, indicating the complete oxidation of graphite [31].

FTIR spectra of GO, Bent-GO and Bent-ErGO were recorded in order to know the possible functional groups. The

characteristic bands (**Fig. 1B a**) due to O-H stretching vibrations at 3435 cm^{-1}, C=O stretching vibrations from carbonyl groups at 1724 cm^{-1}, C=C stretching vibrations at 1618 cm^{-1}, C-O stretching vibrations at 1393 cm^{-1} and vibrations of phenyl hydroxyl groups at 1049 cm^{-1} confirmed the presence of different types of oxygen functionalities on GO [32]. The C=O band was shifted to lower wavelength and intensities of all other bands were decreased upon the modification of GO with Bent (**Fig. 1B b**). Further, the band at 1724 cm^{-1} (**Fig. 1B c**) was almost disappeared with marked decrease in C-O band intensity upon electrochemical reduction of Bent-GO.

UV absorption spectra were recorded to find out the changes before and after electrochemical reduction of GO. The absorption spectra of GO (**Fig. 1C a**) and Bent-GO (**Fig. 1C b**) dispersions exhibited maximum absorption at ~236 nm corresponding to $\pi \rightarrow \pi^*$ transitions of aromatic C-C bonds. After electrochemical reduction of Bent-GO, the absorption maximum was shifted to ~275 nm (**Fig. 1C c**) suggesting that the electronic conjugation within the graphene sheets was restored [33].
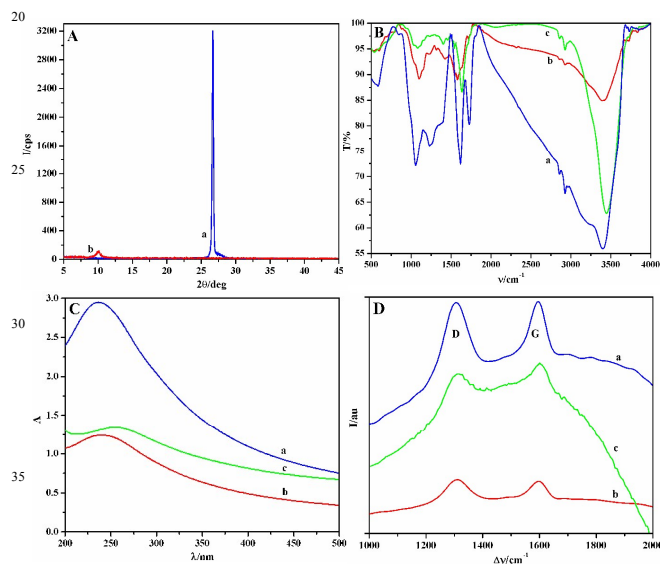
Fig. 1 (A) Powder XRD patterns of pristine graphite powder (a) and graphite oxide (b); (B) FTIR spectra; (C) Absorption spectra and (D) Raman spectra of GO (a), Bent-GO (b) and Bent-ErGO (c).

FT-Raman spectra were recorded to investigate the structural defects of GO, Bent-GO and Bent-ErGO. Raman bands of GO (**Fig. 1D a**), Bent-GO (**Fig. 1D b**) and Bent-ErGO (**Fig. 1D c**) are shown. All graphene oxide derivatives exhibited D and G bands (**Fig. 1D**). The D band at ~1305 cm^{-1} indicated the existence of defective structures in a single-crystal graphene layer and the G band at ~1594 cm^{-1} represented the E_{2g} zone center mode of the crystalline graphite [34]. Further, the relative intensity ratio of D to G bands (ID/IG ratio) reflected the defect density in graphene sheets [34]. This ratio for GO, Bent-GO and Bent-ErGO was found to be 0.996, 0.975 and 1.033 respectively, indicating that many defective sites existed on the surface of Bent-ErGO compared to those on GO derivatives.
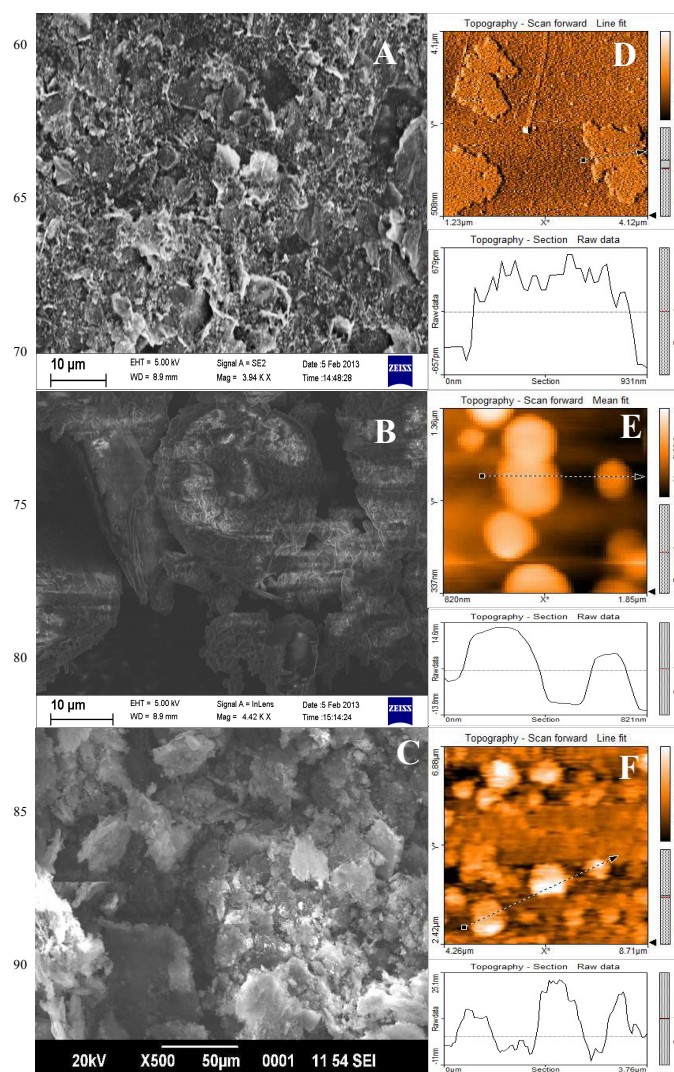
Fig. 2 FESEM micrographs of GO (A), Bent-GO (B) and Bent-ErGO (C). AFM images and their depth profile diagrams of GO (D), Bent-GO (E) and Bent-ErGO (F).

FESEM and AFM are powerful tools to characterize the surface features. In the present work, they were used to obtain the surface morphology and thickness of nanocomposites. The SEM and AFM micrographs of GO, Bent-GO and Bent-ErGO are shown in **Fig. 2.** It was evident from **Fig. 2A** that the GO revealed heterogeneity and consisted of many cavities and crumpled sheets closely associated with each other and formed a disordered solid [35]. Upon modification with Bent, the Bent-GO nanocomposite displayed the uniform accumulation of Bent on GO flakes (**Fig. 2B**). Such homogenous accumulation of Bent on GO was proposed to be favorable for sensor performance due to its intrinsic adsorption property. Upon the electrochemical reduction of Bent-GO, long range nanocomposite GO flakes were broken down into small size puckered flakes (**Fig. 2C**). Flakes type of graphene oxide sheets were observed with the width of each flake of around 3.3 nm (**Fig. 2D**). The observed larger value compared to the reported value of 0.8 nm [12], could be attributed to the presence of individual flakes bearing oxygen-containing functional groups on both faces or to the assembly of

4-5 graphene sheets. The width of GO flakes was increased from 3.3 to 38 nm upon the homogeneous dispersion of Bent (**Fig. 2E**). The average thickness of the nanocomposite film was decreased to ~22 nm upon electrochemical reduction of oxygenated 5 functional groups (**Fig. 2F**).

Characterization of sensing interfaces

The electroactive surface areas of Bent-ErGO/GCE, ErGO/GCE, GO/GCE, Bent/GCE, Bent-GO/GCE and bare GCE were obtained using $K_3[Fe(CN)_6]$ as a probe (data not shown) using the 10 Randles–Sevčik equation shown below:

$$i_p = (2.69 \times 10^5) \, n^{3/2} A D^{1/2} C \, \nu^{1/2}$$

where i_p is the peak current, n is the number of electrons transferred, A is the surface area of the electrode, D is the diffusion coefficient, ν is the scan rate and C is the probe 15 concentration. The electroactive surface area of Bent-ErGO/GCE, ErGO/GCE, GO/GCE, Bent/GCE, Bent-GO/GCE and bare GCE was calculated to be 0.75, 0.67, 0.20, 0.54, 0.39 and 0.051 cm^2 respectively. Thus, larger surface area of Bent-ErGO/GCE facilitated the electron transfer rate.

20 Heterogeneous charge transfer kinetics of bare and modified GCEs were evaluated from the voltammetric data. Cyclic voltammograms of 1 mM $K_3[Fe(CN)_6]$ at Bent-ErGO/GCE (curve a), ErGO/GCE (curve b), Bent-GO/GCE (curve c), GO/GCE (curve d), Bent/GCE (curve e) and bare GCE (curve f) 25 in 1 M KCl are depicted in **Fig. 3A**. The electrochemical characteristics of these electrodes are summarized in **Table 2**. The charge transfer kinetics were observed to be maximum with ErGO/GCE and Bent-ErGO/GCE compared to those observed with other modified GCEs. However, the redox peak current (~77 30 µA) was observed to be highest at Bent-ErGO/GCE compared to that noticed at other modified GCEs and bare GCE. This was attributed to the presence of various defective sites and huge electroactive surface area. This was also supported by Raman (defective sites) spectral studies.

35 EIS was further used to examine the electronic properties of modified electrodes. Results are formatted in the form of Nyquist plot and presented in **Fig. 3B**. The Nyquist plot consisted of semicircle and straight line. The Nyquist plot was fitted with the equivalent circuit model to evaluate the electrochemical 40 characteristics of the interfaces. The charge transfer resistance (R_{ct}), solution resistance (R_s), constant phase element (CPE) and surface heterogeneity (n) of the modified surface were obtained from the semicircle of the Nyquist plot. The semicircular part at higher frequencies corresponds to the charge transfer limited

45 process and the diameter is equivalent to the charge transfer resistance (R_{ct}). The linear part at lower frequencies corresponds to the diffusion process [36]. Nyquist diagrams of 1mM $K_3[Fe(CN)_6]$ at Bent-ErGO/GCE, ErGO/GCE, GO/GCE, Bent/GCE, Bent-GO/GCE and bare GCE in 1 M KCl (**Fig. 3B**). 50 As shown in Nyquist plots, differences in diameters of the semicircle were noticed at different electrodes [Bent-ErGO/GCE (curve a), ErGO/GCE (curve b), Bent-GO/GCE (curve c), GO/GCE (curve d), Bent/GCE (curve e) and bare GCE (curve f)]. From **Fig. 3B**, it was evident that the diameter of the semicircle 55 increased upon the modification of GCE with GO, Bent-GO and Bent. This could be due to change in the apparent charge transfer resistance. Further, no semicircle was observed for Bent-ErGO/GCE and ErGO/GCE suggesting that the spectra were dominated by Warburg impedance and hence the electrochemical 60 processes were diffusion controlled over the whole range of frequencies examined.

The equivalent circuit of the modified electrodes was obtained by fitting the impedance results with standards and the corresponding equivalent circuits are shown as inset of **Fig 3B**. 65 From these fitted circuits various electrical parameters (R_{ct}, R_s, CPE and n) were obtained and the corresponding values are tabulated in **Table 2**. The value of R_{ct} was increased upon the modification of GCE with Bent due to increase in the electrical resistance of the electrode interface. This was reflected in shifting 70 of the oxidation peak towards positive direction at Bent/GCE. Incorporation of GO has improved the charge transfer resistance of the nanocomposite material. Upon reduction, the resistance of GO was reduced. This resulted in the lower charge transfer resistance at ErGO/GCE. Incorporation of Bent with ErGO did 75 not alter the charge transfer resistance of the material at Bent-ErGO/GCE. The roughness factor n was found to be close to unity at Bent-ErGO/GCE. The uniformity of nanocomposite was improved upon the incorporation of Bent. Impedance results are in good agreement with cyclic voltammetric measurements.

80 ### Electrochemical studies of MD at Bent-ErGO/GCE, ErGO/GCE and bare GCE

The applicability of Bent-ErGO/GCE for electrochemical investigations of MD was examined and the results were compared with those obtained at bare GCE and ErGO/GCE. 85 Cyclic voltammograms of 5 µM MD at Bent-ErGO/GCE, ErGO/GCE and bare GCE in phosphate buffer of pH 3 are shown in **Fig. 3C**.

Table 2 Electrochemical characteristics of different modified electrodes

Modified GCE	Voltammetric results*			Impedance spectroscopic results*				
	Surface Area (cm^2)	ΔE_p (mV)	I_p (µA)	R_{ct} (kΩ cm^2)	R_s (Ω cm^2)	CPE (µF cm^{-2})	n	W_0 (kΩ cm^2)
NaB-ErGO	0.748	105	~77.12	0.03	1.04	14.65	0.990	2.05x10^{-4}
ErGO	0.671	103	~57.43	0.02	1.04	7.540	0.721	1.81x10^{-4}
NaB-GO	0.389	161	~37.63	3.79	1.13	2.374	0.712	1.36x10^{-4}
GO	0.202	148	~19.28	3.45	1.13	2.202	0.844	1.38x10^{-4}
NaB	0.545	241	~52.04	11.28	1.13	1.088	0.647	0.39x10^{-4}
Bare GCE	0.0512	106	~32.85	3.151	1.13	3.232	0.738	1.46x10^{-4}

The redox peak current of MD was increased at Bent-90 ErGO/GCE (**Fig. 3B a**) by about 20-fold and 54-fold compared to that at ErGO/GCE (**Fig. 3B b**) and bare GCE (**Fig. 3B c**) respectively. This could be due to the synergetic effect of Bent and ErGO flakes. In other words, the pre-concentration of MD at Bent-ErGO/GCE was higher compared to that at ErGO/GCE due 95 to the presence of various defective sites, huge surface area and the interface with adsorption and intercalation property.

Optimization of conditions for electrochemical determination

Effect of pH

The effect of pH on the electrochemical response of MD at Bent-ErGO/GCE was investigated by CV. From variations in peak currents and peak potentials with pH of the electrolyte (3 - 8) [**Fig. 3D**], it was evident that the oxidation peak current decreased with increase in pH of the electrolyte while the reduction peak appeared only at pH 3 and 4. In addition, the oxidation and reduction peaks were shifted towards negative potentials with increase in pH indicating the participation of protons in the electrode process. A well defined redox peak with enhanced peak currents was observed in phosphate buffer of pH 3. Hence, phosphate buffer of pH 3 was selected for further studies.
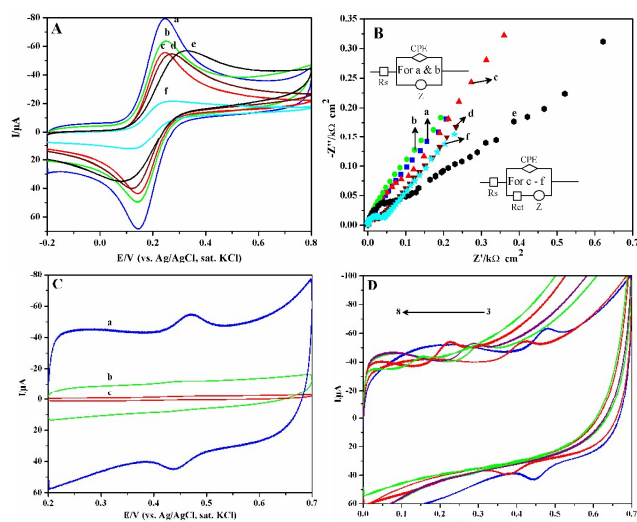
Fig.3 (A) Cyclic voltammograms and (B) Impedance spectra of 1mM [Fe(CN)$_6$]$^{3-/4-}$ at Bent-ErGO/GCE (a), ErGO/GCE (b), Bent-GO/GCE (c), GO/GCE (d), Bent/GCE (e) and bare GCE (f) in 1M KCl; (C) cyclic voltammograms of 5μM MD at Bent-ErGO/GCE (a), Bent/GCE (b) and bare GCE (c) in phosphate buffer of pH 3 and (D) cyclic voltammograms of 5μM MD at Bent-ErGO/GCE in phosphate buffer of diffrent pH.

Effect of modifier and amount of Bent-GO suspension

Modification of GCE with different amounts of modifier (Bent) and GO suspension was investigated by CV. When the amount of Bent in the composite was increased from 0 to 75 %, the response of the electrode improved markedly and showed maximum peak current with 25 % Bent and 75 % GO suspension. Beyond 25 % Bent, the peak current decreased (ESI, Fig.S2†) as the percentage of GO in the electrode material decreased. This was attributed to increased resistance and double layer capacitance of the modified electrode. Therefore, 25 % Bent and 75 % GO was chosen for fabrication of the electrochemical sensor.

The electrochemical signal of MD increased sharply with increase in the amount of Bent-GO suspension and attained maximum with 5 μL. Further, the current did not change significantly with the addition of increasing amounts of Bent-GO suspension (ESI, Fig.S3†). Hence, 5 μL Bent-GO suspension was selected for the preparation of Bent-GO/GCE.

The peak currents of MD increased with increase in accumulation time up to first 120 s. Beyond 120 s, they decreased marginally (ESI, Fig.S4†). This was due to saturation of the modified electrode surface with MD. Hence, the accumulation time of 120 s was chosen for further experiments.

Influence of scan rate

Influence of sweep rate (ν) on the electrochemical behaviour of MD was explored to understand the nature of the electrode process. For this, we have recorded cyclic voltammograms of 5 μM MD on Bent-GO/GCE at different sweep rates (ESI, Fig.S5†). Both anodic and cathodic peak currents increased with increase in ν and exhibited linearity with ν (but not with ν$^{1/2}$) in the range of 10-550 mV s^{-1}. This indicated that the electrochemical process was adsorption controlled. Further, the plots of log i_p vs. log ν yielded the values of slopes for anodic peak (log i_{pa} = 0.971 log ν - 3.906; r = 0.996) and cathodic peak (log i_{pc} = 0.969 log ν- 4.201; r = 0.993). This confirmed the adsorption controlled electrode process.

Calibration curve

Calibration curves were constructed by recording chronoamperogram and differential pulse voltammograms of MD in the range of 1.13 - 40.6 μM and 0.100 – 60.0 μM respectively under optimized conditions (**Fig. 4 A & B**).
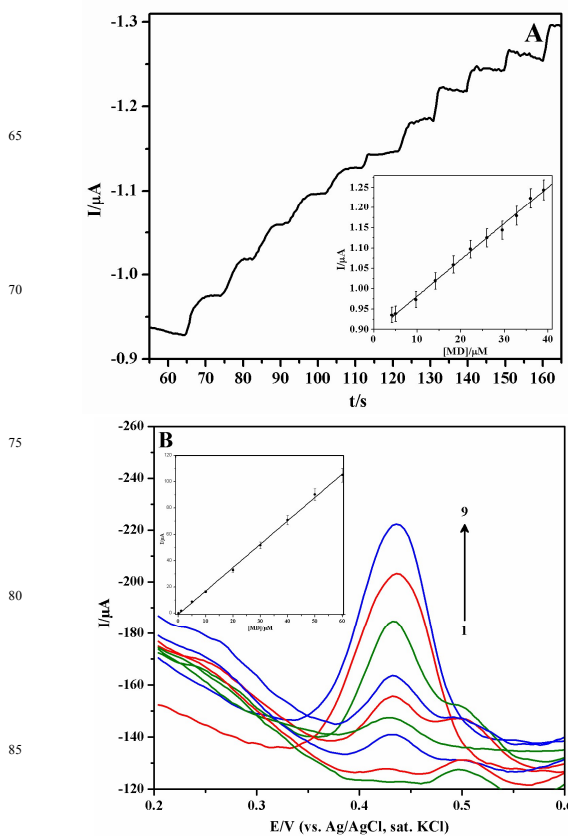
Fig. 4 (A) Chronoamperogram (E$_{pa}$ = 0.534 V vs. Ag/AgCl) for successive addition of MD in the concetration range of 1.13 - 40.6 μM. (B) Differential pulse voltammograms for different concentrations of MD [0.1 (1), 1 (2), 5 (3), 10 (4), 20 (5), 30 (6), 40 (7), 50 (8) and 60 (9) μM] at NaB-ErGO/GCE in phosphate buffer of pH 3. Inset of both (A) and (B) shows linearity plot.

Validation of the optimized procedures for quantitative assay of MD was examined via the evaluation of LOD, LOQ, accuracy, precision and recovery values. The values of LOD and LOQ were

calculated using the equations shown below [37]:

LOD= 3 s / m and LOQ= 10 s / m

where s is the standard deviation of the peak currents of blank (five runs), and m is the slope of the calibration curve. The values of LOD and LOQ were found to be 0.962 μM and 3.19 μM in chronoaperometric method and 0.0403 μM and 0.134 μM in DPV method respectively (ESI, Table S1†). Low values of both LOD and LOQ confirmed the sensitivity of the proposed methods. Inter-and intra-day assay reproducibility of the methods was examined. Results of analyses of these studies yielded RSD values less than 2.04 and 2.83 % for inter-day and intra-day assay, respectively (ESI, Table S1†) confirming good precision of the proposed chronoamperommetric and DPV methods. The major advantages of the proposed methods are their simplicity, ease of performance and sensitivity for the assay of MD compared to reported methods (**Table 1**).

Application of Bent-ErGO/GCE for the determination of MD in pharmaceutical formulations

The proposed electrochemical sensor (using DPV method) was applied for the analysis of MD in pharmaceutical products in order to examine the accuracy and reliability of the proposed method. The corresponding results of tablet analysis are shown in **Table 3**. Known amounts of standard solutions of MD were added to corresponding pre-analyzed tablet solutions to examine the recovery of the proposed method. The results of analysis are tabulated in **Table 3**. The recovery ranged from 98.0 % to 100.04 %, and the RSD (n = 6) values were observed to be less than 2.20 %. Higher percentage of recovery values indicated that the commonly encountered excipients and additives in the formulation did not interfere in the assay of MD by the proposed methods. The low RSD values highlighted the reproducibility of results.

Table 3 Results of analysis of MD in pharmaceutical formulations

	ALDOPA[a]	ALDOMET[b]
Labelled amount, mg	250.00	250.00
Amount found, mg	248.93	248.18
Recovery, %	99.57	99.27
RSD[c], %	0.42	0.72
Pure MD added to tablet solution, mg	25.00	25.00
Amount found, mg	24.50	25.01
Recovery, %	98.00	100.04
RSD[c], %	2.11	2.20

[a]Neon Laboratories Ltd, India.

[b]Merck & Co., Inc.

[c]Average of six determinations.

The results of analysis were compared statistically by the variance ratio F-test and by Student t-test with those obtained by the reported voltammetric method (using carbon nanotube modified carbon-paste electrode and ferrocene as an electro-catalyst) [23]. The calculated F-value (3.99) at 95 % confidence level did not exceed the tabulated value (6.26) indicating that there was no significant difference in precision between the proposed and reported methods. In addition, the calculated Student t-value 1.84 for 0.05 probability level did not exceed the tabulated value (2.13) indicating that there was no significant difference in the accuracy between the proposed and reported methods.

Interference and stability studies

Effects of ascorbic acid, glycine, citrate, glucose, lactose, starch, cellulose, acacia, urea and thiourea were examined in the determination of MD at Bent-ErGO/GCE in order to judge the selectivity of the proposed method. The results of analysis are recorded in **Table 4**. It was noticed that several folds excess of these compounds did not exhibit any influence on the signal of 5 μM MD. This demonstrated that the Bent-ErGO/GCE is selective for the assay of MD.

Table 4 Tolerance of interferences on the determination of 5 μM MD using proposed sensor

Interfering Substance(IS)	Concentration of IS (μg mL^{-1})	Fold	Recovery (%)
Ascorbic acid	5	47	98.91
Glycine	9	86	98.90
Citrate	30	284	96.68
Glucose	60	568	99.22
Lactose	14	132	97.80
Starch	20	189	99.19
Cellulose	15	142	96.37
Acacia	14	132	98.39
Urea	20	189	99.60
Thiourea	15	142	98.35

Storage stability of the Bent-ErGO/GCE was explored by monitoring the peak current of MD kept in air at room temperature. No significant decrease in the peak current on successive two days was observed in the determination of 5 μM MD. Further, 96 % response was observed after three weeks. This indicated the stability of Bent-ErGO/GCE for analytical applications.

Conclusions

A new electrode material, sodium bentonite electrochemically reduced graphene oxide nanocomposite was prepared and used for the development of an electrochemical sensor for the determination of MD. The sensor exhibited a higher electrochemical activity towards the redox response of MD compared to those with ErGO/GCE and bare GCE. The incorporation of sodium bentonite into the graphene oxide suspension followed by electrochemical reduction significantly increased the conductivity and adsorptive property of the electrode interface due to synergetic effect. The proposed electrochemical sensor was successfully applied for the determination of MD in tablets with good precision and accuracy. The proposed method could be used as an alternative method for the assay of MD.

Acknowledgements

Thanks are also due the authorities of the Karnatak University, Dharwad, for providing the necessary facilities.

Notes and references

aDepartment of Chemistry, Karnatak University, Dharwad-580 003, India. E-mail: jseetharam@yahoo.com, drjseetharamappa@kud.ac.in; Fax: +91-836-2747884; Tel: +91 836-221528;
bAnalytical Chemistry Division, Bhaba Atomic Research Centre, Trombay, Mumbai-400 085, India.

‡Results of this work were presented at "32nd Annual Conference of Indian Council of Chemists-2013" (ICC-2013) during 28th - 30th, Nov. 2013 held at Karnatak University, Dharwad.

[1] Y. Liu, X. Dong and P. Chen, *Chem. Soc. Rev.*, 2012, **41**, 2283.
[2] D. C. Marcano, D. V. Kosynkin, J. M. Berlin, A. Sinitskii, Z. Sun, A. Slesarev, L. B. Alemany, W. Lu and J. M. Tour, *ACS Nano*, 2010, **4**, 4806.
[3] Y. Shao, J. Wang, H. Wu, J. Liu, I. A. Aksay and Y. Lin, *Electroanalysis*, 2010, **22**, 1027.
[4] H. Xiong and B. Jin, *J. Electroanal. Chem.*, 2011, **661**, 77.
[5] M. M. I. Khan, A.M. J. Haque and K. Kim, *J. Electroanal. Chem.*, 2013, **700,** 54.
[6] M. A. Raj and S. A. John, *J. Phys. Chem.* C, 2013, **117**, 4326.
[7] K. S. Novoselov, Z. Jiang, Y. Zhang, S. V. Morozov, H. L. Stormer, U. Zeitler, J. C. Maan, G. S. Boebinger, P. Kim and A. K. Geim, *Science*, 2007, **315**, 1379.
[8] K. S. Novoselov, A. K. Geim, S. V. Morozov, D. Jiang, M. I. Katsnelson, I. V. Grigorieva, S. V. Dubonos and A. A. Firsov, *Nature*, 2005, **438**, 197.
[9] S. Park and R. S. Ruoff, *Nat. Nanotechnol.* 2009, **4**, 217.
[10] V. H. Pham, H. D. Pham, T. T. Dang, S. H. Hur, E .J. Kim, B .S. Kong, S. Kim and J. S. Chung, *J. Mater. Chem.*, 2012, **22**, 10530.
[11] V. Mani, A. P. Periasamy and S. M. Chen, *Electrochem. Commun.*, 2012, **17**, 75.
[12] H. C. Schniepp, J. L. Li, M. J. McAllister, H. Sai, M. Herrera-Alonso, D .H. Adamson, R. K. Prud'homme, R. Car, D. A. Saville and I. A. Aksay, *J. Phys. Chem.* B, 2006, **110**, 8535.
[13] H. L. Guo, X. F. Wang, Q. Y. Qian, F. B. Wang and X. H. Xia, *Acs Nano*, 2009, **3**, 2653.
[14] F. Y. Zhang, Z. H. Wang, Y. Z. Zhang, Z. X. Zheng, C. M. Wang, Y. L. Du and W. C. Ye, *Talanta*, 2012, **93**, 320.
[15] A. M. J. Haque, H. Park, D. Sung, S. Jon, S. Y. Choi and K. Kim, *Anal. Chem.*, 2012, **84**, 1871.
[16] A. Fitch, *Clays Clay Miner.*, 1990, **38**, 391.
[17] N. L. Benowitz, (Ed. B. G. Katzung), 9th Ed., McGraw-Hill, New York, 2004.
[18] S. K. Moccelini, A. C. Franzoi, I. C. Vieira, J. Dupont and C. W. Scheeren, *Biosens. Bioelectron.*, 2011, **26**, 3549.
[19] A. Mohammadi, A. B. Moghaddam, R. Dinarvand, J. Badraghi. F. Atyabi and A. A. Saboury, *Int. J. Electrochem. Sci.* 2008, **3**, 1248.
[20] S. Shahrokhian, R. S. Saberi and Z. Kamalzadeh, *Electroanalysis*, 2011, **23**, 2248.
[21] M. Fouladgar and H. K. Maleh, *Ionics*, 2013, **19**, 1163.
[22] M. B. Gholivand and M. Amiri, *Electroanalysis*, 2009, **21**, 2461.
[23] A. Salmanipour, M. A. Taher and H. Beitollah, *Anal. Methods*, 2012, **4**, 2982.
[24] H. K. Maleh, M. A. Khalilzadeh, Z. Ranjbarha, H. Beitollahi, A. A. Ensafi and D. Zareyee, *Anal. Methods*, 2012, **4**, 2088.
[25] Z. Talebpour, S. Haghgoo and M. Shamsipur, *Anal. Chim. Acta.*, 2004, **506**, 97.
[26] L. K. Abdulrahman, A. M. Al-Abachi and M. H. Al-Qaissy, *Anal. Chim. Acta*, 2005, **538**, 331.
[27] T. Matthieu, C. D, Debora and A. R. Jose, *Anal. Lett.*, 2006, **39**, 327.
[28] H. He, Q. Zhou, W. N. Martens, T. J. Kloprogge, P. Yuan, Y. Xi, J. Zhu and R.L. Frost, *Clays Clay Miner.*, 2006, **54**, 689.
[29] W.S. Hummers and R.E. Offeman, *J. Am. Chem. Soc.* 1958, **80**, 1339.
[30] S. N. Prashantha, N. L. Teradal, J. Seetharamappa, A. K. Satpati and A. V. R. Reddy, *Electrochim. Acta*, 2014, **133**, 49.
[31] N. L. Teradal, S. N. Prashanth and J. Seetharamappa, *Anal. Methods*, 2013, **5**, 7090.
[32] K. J. Huang, D. J. Niu, J. Y. Sun, C. H. Han, Z. W. Wu, Y. L. Li and X. Q. Xiong, *Colloids Surf. B*, 2011, **82**, 543.
[33] D. Li, M. B. Muller, S. Gilje, R. B. Kaner, G. G. Wallace, *Nat. Nanotechnol.*, 2008, **3**, 101.
[34] N. L. Teradal, S. N. Prashanth, J. Seetharamappa and A.K. Satpati, *Electroanalysis*, 2014, **26**, 2173.
[35] S. Stankovich, D. A. Dikin, R. D. Piner, K. A. Kohlhaas, A. Kleinhammes, Y. Jia, Y. Wu, S. T. Nguyen and R.S. Ruoff, *Carbon*, 2007, **45**, 1558.
[36] A. J. Bard and L. R. Faulkner, *Electrochemical Methods, Fundamentals and Applications*, 2nd Ed. Wiley, NewYork, 2001.
[37] S. Skrzypek, W. Ciesielski, A. Sokolowski, S. Yilmaz, D. Kazmierczak, *Talanta*, 2005, **66**, 1146.

Analytical Methods Accepted Manuscript